

Phase Transitions in Packet Traffic on Regular Networks: a comparison of source types and topologies

D.K. Arrowsmith,^{*} R.J. Mondragón †, J.M. Pitts†, M. Woolf^{*}

October 14, 2004

Keywords: Packet traffic, regular networks, congestion, long-range and short range dependence sources.

Abstract

We extend the packet traffic network models developed in recent years for rectangular grids to other regular networks, and to fragmented networks. The packet transfer mechanism is open-loop as before. The nodes of the network are either hosts or routers. Both can receive and transmit packets towards their destination; hosts can also create and receive packets. Long range dependent traffic with varying Hurst parameter is introduced at the host nodes of these networks, and comparative studies of the onset of congestion are carried out. Results show statistical robustness when the rectangular grid is adapted to form other regular networks. Qualitative behavior is the same, and simple mean field models accurately predict critical points as in the rectangular case. R/S -statistics show the presence of long range dependence even when sources are short range dependent. Results indicate that this long range dependence is closely linked to the queuing mechanism.

1 Introduction

In 1993 Leland *et al.*, [9], demonstrated the presence of *Long Range Dependence* (LRD) in traces of packet traffic rates. They studied Ethernet local area network (LAN) traffic, but subsequent work [17] has shown that LRD also occurs in wide area networks (WAN). LRD causes bursts in the packet rate for a given communication channel.

^{*}School of Mathematical Sciences, Queen Mary, University of London, London E1 4NS, UK.

[†]Dept. of Electronic Engineering, Queen Mary, University of London, London E1 4NS, UK.

This *bursty* behavior occurs over several orders of time scale. Packet traffic was simulated using Poisson processes before the discovery of LRD. Such assumptions are appropriate for modelling voice based traffic, but they produce memory-less, *short range dependent* traffic and are not suited to modelling *LRD*. In the Poisson case overall average packet rates can be accurately predicted from a relatively small set of measurements. The bursty nature of LRD traffic means that an overall average value cannot be accurately determined even when quite a large number of measurements are made. We have shown in [16] that, given the same load on a rectangular grid network, LRD traffic causes an earlier onset of congestion when compared with Poisson traffic; and that the point at which congestion begins is much less well defined. For these reasons we have again used chaotic dynamics ([3]) to model LRD sources. As before, we have compared our results with those obtained when using Poisson sources.

A simple model of network packet traffic across rectangular lattices was introduced by Solé and Valverde. This was the model that was used in [16]. Solé and Valverde, [13] showed that the time series of queue lengths at an arbitrarily selected node in this network was long range dependent. Since the sources were all SRD, this LRD was caused purely by network behavior. This phenomenon was investigated further in [16].

1.1 Long range dependence

The autocorrelation decay, γ_k , for time lag k , of a discrete binary time series X_t , $t \in 0, 1, 2, \dots$, is said to be *long-range dependent* if:

$$\gamma_k \sim ck^{-\beta}, \quad (1)$$

where $\beta \in (0, 1)$, c is a constant, and

$$\gamma_k = \frac{E(X_t X_{t+k}) - E(X_t)E(X_{t+k})}{\sqrt{V(X_t)}\sqrt{V(X_{t+k})}}, \quad (2)$$

$E(\cdot)$ is the expectation or mean value, and $V(\cdot)$ is the variance. The self-similar nature of the LRD traffic is formally defined in [4]. The autocorrelation of SRD traffic

decays *exponentially* rather than as a power law, with the asymptotic behavior given by:

$$\gamma_k \sim C\alpha^{-k} \quad (3)$$

Here $\alpha \in (0,1)$ and C is a constant. The nature of LRD traffic is often expressed using the *Hurst parameter*, $H \in [0.5, 1]$ (see [8]) where $H = 1 - \beta/2 \in (1/2, 1)$, [4]. For SRD traffic $H \rightarrow 1/2$ and the various levels of LRD traffic occur for H increasing in $(0.5, 1]$.

The difference in the behaviour of SRD and LRD data for batched segments of size N is shown in [16]. Define

$$X_m^{(N)} = \frac{1}{N} \sum_{n=mN}^{(m+1)N-1} X_n, \quad (4)$$

for $m = 0, 1, 2, \dots$. The standard deviation in $X_m^{(N)}$ for the *SRD* traffic varies as the square root of the batch size N , whereas it varies as a lower power than square root for LRD traffic. This shows the bursty nature of LRD traffic. Even when averaging over very large batch sizes, uninterrupted sequences of either ‘1’s or ‘0’s may still be longer than the batch size, giving the extreme values and the resulting high variance shown in these plots.

We show in this paper that for the same traffic loads, higher Hurst parameters increase the queue lengths dramatically in triangular and hexagonal lattice models, as was the case for rectangular grids in [16]

1.2 Nonlinear modelling of LRD

We use the *Erramilli* traffic map defined in [16, 3], to provide binary sequences that model host packet production. The output ‘1’ indicates that a packet is added to the host queue for transmission; ‘0’ indicates that no packet is produced. The map f is defined on the unit interval of real numbers $I = [0, 1]$. The iteration of f with an initial value x_0 produces an *orbit* $\{x_n\}$ defined by $x_{n+1} = f(x_n)$ in I , for $n = 0, 1, 2, \dots$. The sequence $\{x_n\}$ in I is converted to binary output z_n by associating the symbols ‘1’ and ‘0’ with the intervals $[0, d]$ and $(d, 1]$ respectively.

The *Erramilli* maps, [3], $f = f_{(m_1, m_2, d)} : I \rightarrow I$, are defined by

$$f(x) = \begin{cases} x + (1-d)(x/d)^{m_1}, & x \in [0, d], \\ x - d((1-x)/(1-d))^{m_2}, & x \in (d, 1], \end{cases} \quad (5)$$

Here $d \in (0, 1)$ and the parameters $m_1, m_2 \in [3/2, 2]$ induce *intermittency*, of order m_1 and m_2 , at the points $x = 0$ and $x = 1$ respectively. The graph of the map f consists of two segments and each has a tangency with the line $y = x$, [16]. The iteration of the map f with initial condition x_0 forms a ‘web’ generating the iterative sequence, or orbit, x_n , where $x_n = f(x_{n-1})$, $n = 1, 2, \dots$

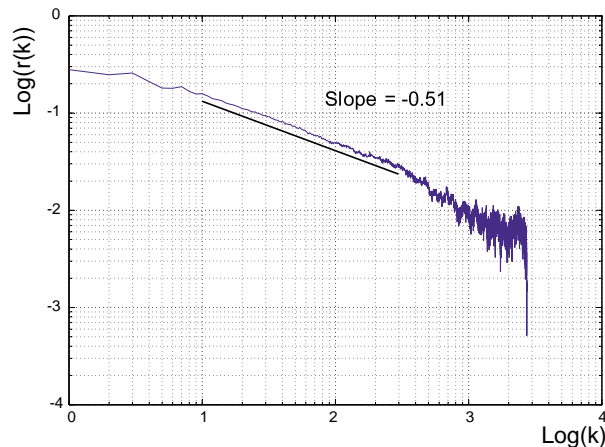


Figure 1: Autocorrelation output for the intermittency map in given by eqn. 5 with $m = 1.5$. The log-log graph for γ_k vs. k agrees with the predicted asymptotic slope for which $H = 1/2$ which is indicated by the thickened line.

Note that the tangencies at $x = 0, 1$ gives a ‘slow’ change in the values of the sequence x_n , and therefore the output z_n provides long sequences of consecutive ‘0’s or ‘1’s.

The intermittency produces slowly incrementing streams of orbital values, [12]. This, in turn, ensures the so-called ‘memory’, or *LRD*, in the digital output z_n . It has been shown that the autocorrelation of the output function z , $\gamma_k \sim k^{-\beta}$, $k \in \mathbf{Z}^+$, has the decay constant $\beta = (2 - m)/(m - 1) \in (0, 1)$ with $m = \max\{m_1, m_2\}$, [7, 10]. This in turn implies that the Hurst parameter $H = (3m - 4)/(2m - 2)$. Hence an appropriate selection of m enables the generation of traffic with any desired H value.

2 Network structures

The basic model we consider here, [13], has a lattice network of interconnected nodes which are either *hosts* or *routers*. All nodes can transfer packets and, additionally, hosts can both transmit and receive packets. Both types of node have buffers for storing packets. Packets when produced are allocated another host *destination* which is chosen randomly. When a packet arrives at the head of a buffer, it is then transferred to the queue at an adjacent node which is closer to its destination. We consider performance factors such as average delivery time of packets and the throughput of packets for this model below. Several network topologies have been studied.

2.1 Routing Algorithms

A routing algorithm is needed to model the dynamic aspects of the network. Packets are created at source hosts and sent through the lattice one step at a time until they reach their destination host. In real packet-switching networks, packets carry header and information payloads with them. They may also carry information about the state of the network. To simplify the modelling, we record only the time of creation and the source and destination addresses when passing packets through the network. No information about the network state is carried.

The routing algorithm operates as follows:

- first a host creates a packet using either a uniform random distribution (Poisson) or a distribution defined by a chaotic map (*LRD*), as described in section 1.
- if a packet is generated it is put on the end of the queue for that host. This is repeated for every host in the lattice.
- packets at the head of each queue are sent to a neighboring node which is closer to the destination node (using the least used link if necessary). If nodes are equidistant from the destination, and link usage is equal, a random selection is made.

This process is repeated for each node in the lattice. The whole procedure of packet generation and movement represents one time step of the simulation. There is no feedback applied to queue lengths in this algorithm and hence the model is uncontrolled.

2.2 Regular and Depleted Lattices

A first model for the study of global network traffic is also discussed in [13],[11], [6], and most recently in [16]. The network takes the form of a rectangular (R) lattice in which each node has four neighbors. This is also known as a *Manhattan* lattice. The finite rectangular lattice \mathcal{Z} consists of L^2 nodes. The position of each node in the lattice \mathcal{Z} is given by the coordinate vector $\mathbf{r} = (i, j)$ where i and j are integers in the range 1 to L .

We use periodic boundary conditions and hence the network can be seen as having a toroidal topology in which nodes on one edge of the lattice are connected to nodes on the opposite edge. To measure the distance between a pair of nodes in the doubly-periodic ‘Manhattan’ lattice \mathcal{Z} , the metric

$$d_R(\mathbf{r}_1, \mathbf{r}_2) = L - \left| |i_2 - i_1| - \frac{L}{2} \right| - \left| |j_2 - j_1| - \frac{L}{2} \right|. \quad (6)$$

is used, where the points $\mathbf{r}_1 = (i_1, j_1)$ and $\mathbf{r}_2 = (i_2, j_2)$ of \mathcal{Z} give the positions of the two nodes.

Each node has a queue of unlimited length in which to store packets.

The hexagonal (H) and (T) and triangular lattices are shown in Fig. 2. Note that the H and T lattices can be

obtained from the R lattice by the removal and addition of edges. Thus the lattices are embedded on the torus in such a way that the edge sets, $e(\cdot)$ of the H, R and T networks satisfy the set inclusions $e(H) \subset e(R) \subset e(T)$, (see Fig. 2). The metrics d_T and d_H for the distance between the two nodes in the T and H lattices cannot be so simply stated as for the rectangular case, but do satisfy the rule:

$$d_T(\mathbf{r}_1, \mathbf{r}_2) \leq d_R(\mathbf{r}_1, \mathbf{r}_2) \leq d_H(\mathbf{r}_1, \mathbf{r}_2)$$

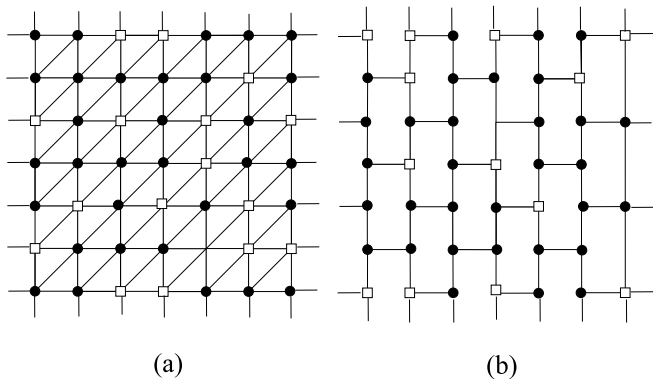


Figure 2: (a) The triangular, and (b), the hexagonal lattices are obtained from the underlying rectangular grid by respectively adding and subtracting edges.

We can also consider depleted networks. In these edge removals have been made from the rectangular lattice, creating irregularity in the node degrees. The edge connections are retained independently with a probability p for each edge. Probabilities larger than $\frac{1}{2}$ are best used as the percolation threshold for an infinite connected network is $p_c = \frac{1}{2}$. Study of these depleted networks is an intermediate step in extending the work to other irregular networks, especially scale-free networks, see [1].

2.3 Hosts and Routers and Traffic Generation

The *density* of hosts $\rho \in [0, 1]$ is the ratio between the number of hosts and the total number of nodes in the network. Hosts are randomly distributed throughout the network and we fix $\rho = 0.164$ for the initial simulations considered here, although a range of ρ values have been considered to confirm that the results are robust.

Incremental change from SRD to LRD traffic can be considered by adjusting the intermittency parameters m_1, m_2 . For simplicity the m_1, m_2 are kept equal to a value $m \in [1.5, 2]$. It should be noted that when the exponents differ, the strongest intermittency dominates the auto-correlation behavior, [7, 10]. Poisson-like traffic is independently created by repeatedly choosing randomly a

number on the interval $[0, 1]$. If it is below a discriminator value $d \in (0, 1)$, then a packet is emitted. Hence, for a uniform distribution, the average rate at which packets are produced at a host is $\lambda = d$. As in previous simulations, we have used the same value of λ for all sources.

3 Onset of Congestion

We have used two performance indicators to study the onset of congestion. The first is *average packet lifetime* ($\langle \tau \rangle$). This is the average time spent by packets in the network. The packet lifetime includes the time taken in travelling from source to destination, and the time spent waiting in queues en route. The second is the throughput which is the ratio of packets delivered to packets created. In [13] and [16] $\langle \tau \rangle$ was seen to increase dramatically as the load was increased. This type of rapid change can be best described as a *phase transition*, [2, 5, 11], in this case from a *free* phase to a *congested* phase. As load is further increased a *critical load* λ_c is reached. This is the point at which the throughput of packets *decreases* as load *increases*. In the following sections we study a variety of different lattice types. End effects are present in all experiments, so run lengths are all the same to make direct comparisons possible.

3.1 Triangular, Rectangular and Hexagonal Lattices

Different traffic sources are compared in a rectangular toroidal lattice, as used in [16]. The host density $\rho = 0.164$. In Fig. 3, $\langle \tau \rangle$ is plotted against the load λ . The sources at the hosts are Poisson and LRD with different values of H . The nature of the traffic changes from *SRD* at $m = 1.5$ ($H = 0.5$) to full *LRD* at $m = 2$ ($H = 1$).

A key observation in [16] (see Fig 3(a)) is the corresponding behavior of LRD traffic for increasing load levels. The statistic $\langle \tau \rangle$ is almost the same as for SRD traffic for $\lambda > \lambda_c$. However, for $\lambda < \lambda_c$ the behavior of $\langle \tau \rangle$ is far more erratic, and does not have the sharp phase transition of the SRD traffic. Average lifetimes in this region can be an order of magnitude greater. This makes the prediction of $\langle \tau \rangle$ for LRD traffic almost impossible at low load levels.

In Fig. 3(b) throughput is plotted against λ for the same types of source. The peak in throughput occurs at the critical point. This is also where the network reaches its peak efficiency. The peak value of throughput is slightly lower for the *LRD* sources, emphasizing the longer lifetimes of packets. However, the difference is less pronounced than that seen in average lifetimes. Away from the peak, values of throughput for the two types of traffic source are very similar. For the T and

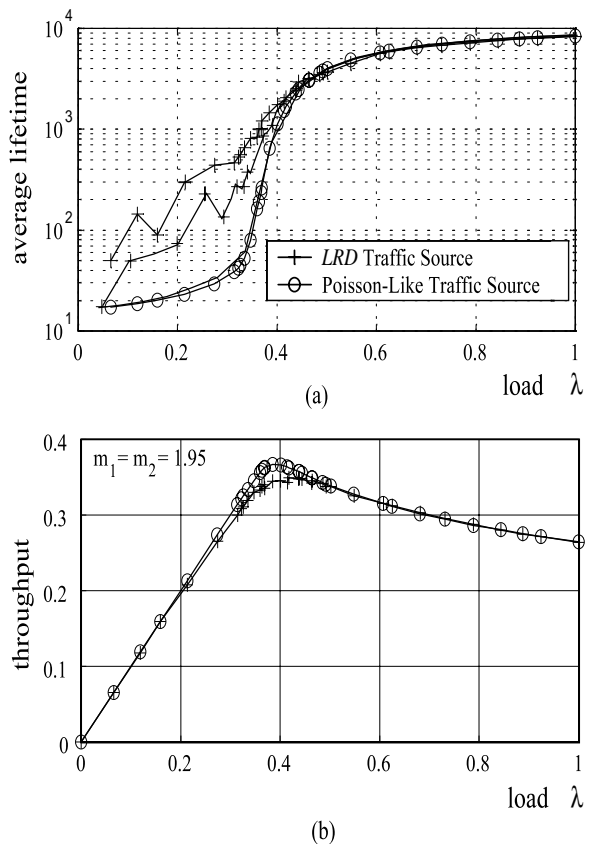


Figure 3: (a) The phase change in $\langle \tau \rangle$ for SRD traffic as the load λ is increased in a rectangular toroidal grid, see [16]. A relatively smooth transition to congestion is shown for the Poisson sources. (b) The corresponding response of throughput to introducing LRD as the Hurst parameter from $H = 0.5$ to $H = 0.9$.

H lattices the qualitative behavior as the networks become congested is the same as for the rectangular lattice. Comparisons are shown in Fig. 4 shows the corresponding plots for T in Fig. 4(a,b) and for H in Fig. 4(c,d) lattices respectively. In the case of the hexagonal lattice the critical point is below the Manhattan value and for the triangular lattice it is above. This is not surprising as the hexagonal lattice has 3 connections per node and therefore lower carrying capacity, whereas the triangular has 6 connections per node, and hence a higher carrying capacity. This critical behavior is discussed in more detail in section 4.

3.2 Depleted Rectangular Lattice

Depleting the lattice has the effect of greatly reducing the number of possible paths in the network, and increasing

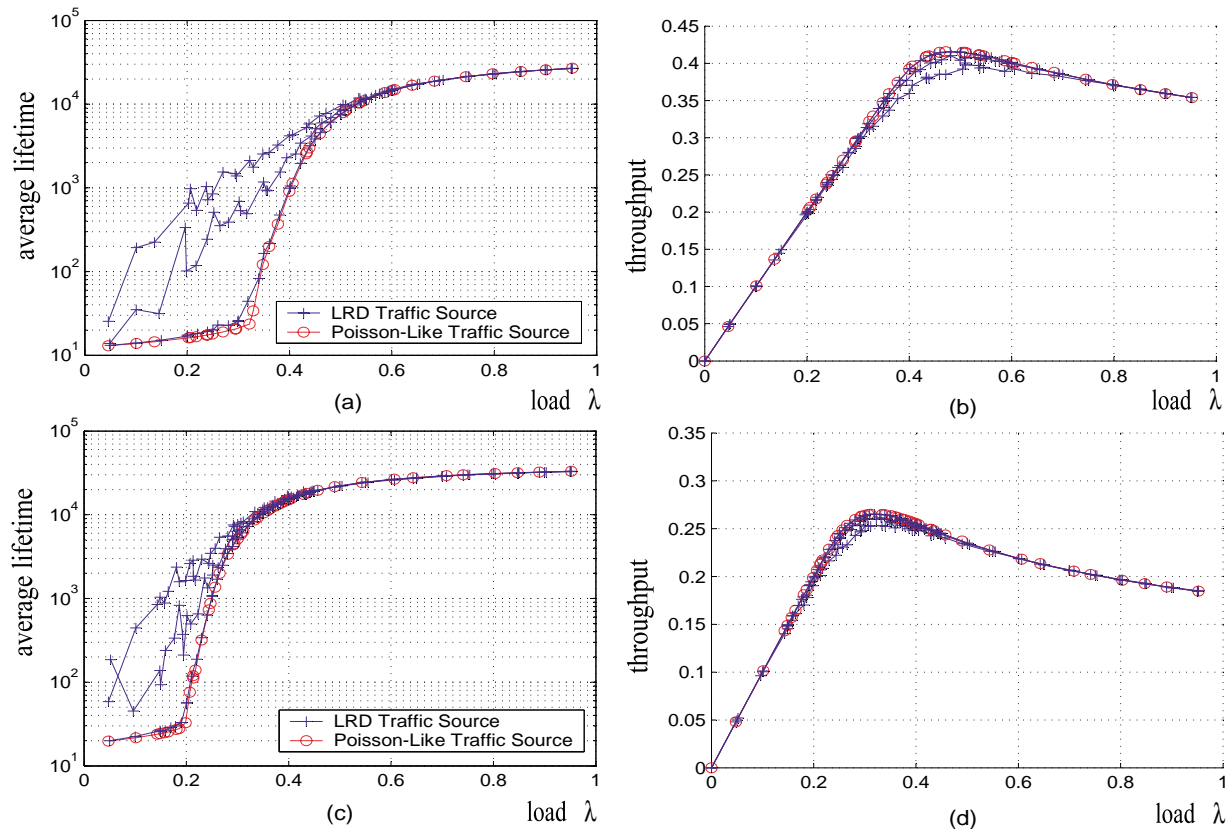


Figure 4: (a) The packet lifetime $\langle \tau \rangle$ and (b), the throughput for SRD and LRD traffic as the load λ is increased in the triangular toroidal grid. (c) The packet lifetime $\langle \tau \rangle$ and (d), the throughput for SRD and LRD traffic as the load λ is increased in the hexagonal toroidal grid. The SRD traffic is obtained by setting $m_1 = m_2 = 1.5$ and the LRD has two values $m_1 = m_2 = 1.8$ and $m_1 = m_2 = 1.95$.

the average queue lengths. This effect is accentuated by the simple routing algorithm which only allows shortest paths. The reduced numbers of paths lead to relative congestion in the routers along the paths between hosts. Hence routers become congested before hosts, which is the opposite case to that of all the regular lattices. Congestion also occurs at much lower loads for the depleted lattice.

4 Mean Field Models

Simple mean field models have been developed, [13, 16], to describe the global network performance in rectangular grids below the critical point. We show that a simple extension of the concept to other regular networks can be used to give the different critical values.

The critical load λ_c can be estimated by looking at the total distance that all the packets at time t have to travel to reach their destination. Consider the congested phase in which there are queues at all nodes. Then the

change in the total distance traveled by packets in one time step of the simulation is:

$$D(N_{t+1}) - D(N_t) \quad (7)$$

where N_t is the number of packets in the queues at time t and $D(N_t)$ is the aggregate distance of all these packets from their destinations at time t . The number of packets in the network increases by $\rho\lambda L^2$ in the time step. Let d_{av} be the average distance to destination on a given lattice, then $d_{av}(L) = L/2$ for the R-lattice, $d_{av}(L) \sim 0.39L$ for the T-lattice, and $d_{av}(L) \sim 0.55L$ for the H-lattice as $L \rightarrow \infty$. Hence the overall distance added by packets entering the network is $\rho\lambda L^2(d_{av}(L))$. In contrast, the aggregate distance is reduced by L^2 , since every packet at the head of the queue moves one step closer to its destination. Thus the change in total distance to destination between time t and $t + 1$ is:

$$D(N_{t+1}) - D(N_t) = \rho\lambda L^2(d_{av}(L)) - L^2. \quad (8)$$

The critical load λ_c occurs when the total distance no

longer decreases giving

$$\lambda_c = 1/\rho d_{av}(L) \quad (9)$$

for the various lattices. This result was obtained for the R-lattice (for the special case $\rho = 1$) in [6]. It should be noted that as ρ increases, typically the total load on the system increases and the phase transition becomes sharper. Estimating the load at which congestion begins, $\lambda'_c < \lambda_c$ requires a more sophisticated derivation and is obtained by taking into account differences between the host and router traffic. In [16] we derived the formula

$$\lambda'_c = 1/(\rho \frac{L}{2} - \rho + 1) \quad (10)$$

where λ'_c is called the *local critical point*. This can be trivially extended to the other regular grids as

$$\lambda'_c = 1/(\rho d_{av}(L) - \rho + 1). \quad (11)$$

4.1 Mean field critical behavior

The accuracy of the mean field model described above is illustrated in Fig. 5. As was found for the rectangular lattice in [16], the prediction of critical load λ_c agrees very well with the simulation for both the hexagonal and triangular lattices. The estimation of local critical load, λ'_c is good, but the quality of the approximation decreases with the connectivity of the lattice. The values of λ_c reduce as the connectivity of the network decreases, with the hexagonal lattice having the lowest λ_c . However, the quality of the mean field assumptions appears to depend on the regularity of the networks and breaks down when depleted lattices are considered. In particular, there is strong evidence that the mean field approach becomes an increasingly poor predictor of criticality at low loads for depleted regular graphs. The underlying regularity of the lattice seems to be an essential part of the successful modelling.

5 R/S measurements

Rescaled range statistical analysis, R/S analysis, is one of a number of methods used for estimating the Hurst parameter H . It is described in [4].

In tables 1, 2 and 3 we show H values obtained with R/S analysis for the three regular networks using Poisson-like sources. Host densities and network size are the same for all three cases. The network topologies differ only in the degrees of each node. The degrees are 6 for the T-lattice, 4 for the R-lattice and 3 for the H-lattice. Three time series have been studied:

- the average host queue length at each time step;

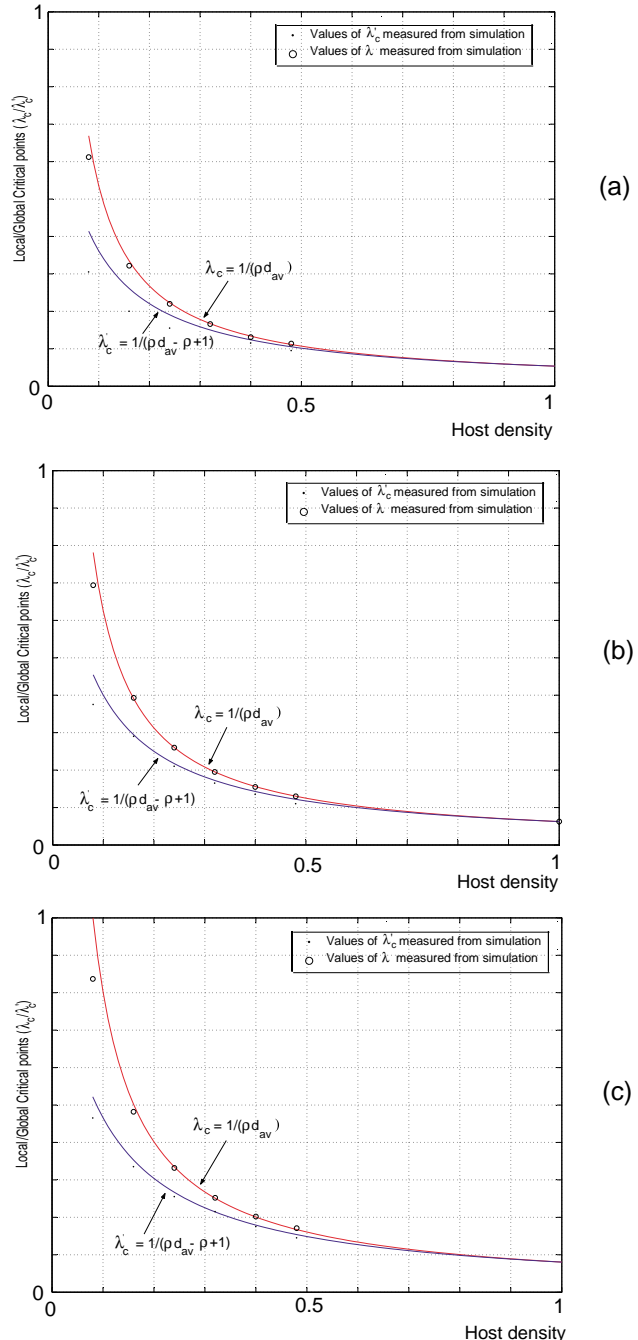


Figure 5: Mean field approximation for critical load λ_c showing strong agreement with numerical simulations for the (a) triangular, (b) rectangular lattice, and (c) hexagonal lattice. The onset of the critical load λ'_c is also indicated although the quality of this approximation decreases with connectivity. Note the critical load $\lambda = \lambda_c$ reduces through the graphs (a),(b),(c) reflecting the decreasing connectivity $T \rightarrow R \rightarrow H$.

- the average router queue length at each time step;
- and the total number of packets leaving the network at each time step.

For each lattice type, three λ values below the local critical point have been chosen: one well below the local critical point; one slightly below; and one very close to this threshold, but still below this value. Time series for these load values are all steady state. The abbreviations are AHQL - Average host queue lengths; ARQL - Average router queue; PLS - Packets leaving system.

Table 1: H values for the H- hexagonal lattice with Poisson-like sources. Three time series have been analyzed: average host queue lengths at each time step, average router queue lengths at each time step and the number of packets leaving the network at each time step.

Load(λ)	AHQL	ARQL	PLS
0.10	0.61	0.66	0.53
0.18	0.70	0.71	0.53
0.195	0.86	0.69	0.53

Table 2: H values for the R- rectangular lattice with Poisson-like sources. The time series analyzed are the same as in table 1.

Load(λ)	AHQL	ARQL	PLS
0.10	0.61	0.64	0.53
0.27	0.84	0.76	0.53
0.29	0.92	0.76	0.53

Table 3: H values for the T- triangular lattice with Poisson-like sources. The time series analyzed are the same as in table 1.

Load(λ)	AHQL	ARQL	PLS
0.10	0.60	0.61	0.53
0.30	0.75	0.68	0.52
0.33	1.00	0.70	0.53

Time series of the packets leaving the network always have the Hurst parameter $H \approx 0.5$. That is to say none of them exhibit LRD. The time series of average queue lengths, however, all show some degree of LRD. H values rise sharply close to the local critical point, especially for the hosts (where congestion occurs first). Very close to the local critical point they approach 1 for host queues for all the regular topologies.

The fact that this behavior only occurs in queues suggests that the self-similarity is closely linked to the queuing mechanism.

6 Conclusions

In this paper we have extended our previous work, [16], by considering different topologies of networks. The T- and H- lattices can be seen to be part of the same family as the rectangular lattice by set inclusion and so robustness of results on congestion have been assessed - in particular the critical load parameters increase with the sparseness of the network.

The mean field models, both for critical and local critical point work well for the new regular topologies. This breaks down for the depleted lattice. The path to congestion for this network is clearly fundamentally different to that of the regular networks.

We have seen LRD in networks with purely SRD sources in this work and also in [13] and [16]. However high H values have only been seen in measurements of queue lengths near or above the local critical point. This suggests that the queuing mechanism is the predominant factor. This requires further investigation.

In our current work we aim to model real networks, especially the internet, more closely. This requires the modelling of a packet transfer mechanism that includes feedback, and the move to a more realistic network topology, see [1].

ACKNOWLEDGEMENT One of the authors(DKA) would like to thank the organisers of the *Mathematical Perspectives of Teletraffic Theory Workshop* at Institut Mittag-Leffler, Stockholm for his stay during the preparation of this paper.

References

- [1] M. Woolf, D.K. Arrowsmith, R.J. Mondragón, J.M. Pitts and S. Zhou, Dynamical modelling of TCP packet traffic on scale-free networks, *preprint*.
- [2] R. Albert and A-L Barábasi, Statistical Mechanics of Complex Networks, *Rev. Mod. Phys.* **74**, 47 (2002), also *arXiv:cond-mat/0106096*, 1-54.
- [3] A. Erramilli, R.P. Singh and P. Pruthi, Chaotic maps as models of packet traffic, *Proc. 14th Int. Teletraffic Conf. 1994*, North-Holland(Elsevier), 329-38.
- [4] J. Beran, Statistics of long memory processes, *Monographs on Stats and Appl. Prob.* **61**, Chapman & Hall, London.

- [5] K.Fukuda, H.Takayasu, and M.Takayasu, Origin of Critical Behavior in Ethernet Traffic, *Physica A* **287**, 2000, 289-301.
- [6] H. Fuks and A.T. Lawniczak, Performance of data networks with random links, *Math and Computers in Simulation*, **51** 1999, 101-17.
- [7] A. Giovanardi, G. Mazzini, and R. Rovatti, Chaos based self-similar traffic generators, *Proc. NOLTA 2000*, 747-50.
- [8] H.E. Hurst, Long-range storage capacity of reservoirs, *Trans Am. Soc. Civ. Eng.* **116**, 1951, 770-99.
- [9] W.E. Leland, M.S. Taqqu, W. Willinger and D.V. Wilson, On the Self-Similar Nature of Ethernet Traffic, *Proc ACM SIGCOMM 93*, 1993.
- [10] R.J. Mondragón, A model of packet traffic using a random walk, *Int. Jnl of Bif. and Chaos*, **9**(7), 1381-92, 1999.
- [11] T. Ohira and R. Sawatari, Phase transition in a computer network traffic model, *Phys. Rev. E* **58** 1998, 193-95.
- [12] H.G. Schuster, *Deterministic Chaos: An Introduction*, 3rd Edition VCH, 1995.
- [13] R. V. Solé and S. Valverde, Information transfer and phase transitions in a model of internet traffic, *Physica A* **289**, 2001, 595-605.
- [14] X-J Wang, Statistical physics of temporal intermittency, *Phys Rev A* **40**(11), 1989, 6647-61.
- [15] S. Zhou and R.J. Mondragón, Towards modelling the Internet Topology - the Interactive Growth Model, *preprint, Dept. of Elec. Eng., QM, University of London*.
- [16] M. Woolf, D.K. Arrowsmith, R.J. Mondragon, J.M. Pitts, Optimization and Phase Transitions in a Chaotic Model of Data Traffic, *Phys Rev E* **66**, 046106 (2002).
- [17] V. Paxson and S. Floyd, Wide-Area Traffic: The Failure of Poisson Modeling, *IEEE/ACM Trans. on Networking*, **3**,no. 3, 1995, 226-244.